

Ortho Effect in the Bergman Cyclization: Electronic and Steric Effects in Hydrogen Abstraction by 1-Substituted Naphthalene 5,8-Diradicals

Frank C. Pickard IV, Rebecca L. Shepherd, Amber E. Gillis, Meghan E. Dunn, Steven Feldgus, Karl N. Kirschner, and George C. Shields*

Department of Chemistry, Hamilton College, Clinton, New York 13323

Mariappan Manoharan and Igor V. Alabugin*

Department of Chemistry and Biochemistry, Florida State University, Tallahassee, Florida 32306-4390

Received: October 31, 2005; In Final Form: December 9, 2005

We present a detailed theoretical study of geometries, electronic structure, and energies of transition states and intermediates completing the full Bergman cycloaromatization pathway of ortho-substituted enediynes with a focus on polar and steric contributions to the kinetics and thermodynamics of hydrogen abstraction. This study provides a rare unambiguous example of remote substitution that affects reactivity of a neutral reactive intermediate through an σ framework.

Introduction

The transformation of (Z)-3-ene-1,5-diyne into reactive 1,4-benzene σ,σ -diradicals (*p*-benzynes)¹ (the Bergman cyclization, Scheme 1) have found practical applications in the development of anticancer drugs² and sequence specific DNA mapping tools³ as well as organic⁴ and polymer⁵ synthesis. Success of these applications depends on control over enediyne reactivity through either strain^{6–9} or electronic effects.^{10–14} Unfortunately, because the developing radical centers are orthogonal to the aromatic π -system,^{15,16} neither benzannulation itself nor the nature of para substituents in the annealed benzene ring has a large effect on the cyclization rate.^{13,17}

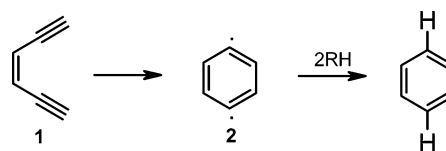
Recently, we suggested that a more efficient way to control the Bergman cyclization involves interaction of the *in-plane* acetylenic orbitals with spatially proximal ortho substituents (Scheme 2).¹⁷ This interaction can be either destabilizing (steric) or stabilizing (hydrogen-bonding/hyperconjugation/electron-transfer) and provides a convenient way to control the activation energies of the Bergman cyclization of benzannulated enediynes.

Role of H-Abstraction in the Bergman Cycloaromatization Cascade

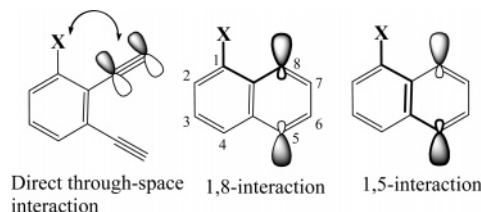
However, the cyclization step is only the first part of the Bergman cycloaromatization cascade, which also includes two hydrogen abstraction steps from a suitable donor. The hydrogen abstraction step is especially important in benzannulated enediynes where the Bergman cyclization is approximately 10 kcal/mol more endothermic than that of the parent enediynes and, thus, the barrier for the retro-Bergman ring opening of *p*-benzyne is small¹⁸ (k_{-1} is large). As a result, the rate of cyclization of benzannulated enediynes depends on the H-atom donor concentration.^{19,20} We developed a simple kinetic model (eq 1, Scheme 3) that describes very well the effects of the relative rate of H-atom abstraction on the rate of disappearance for the enediyne reactant.²¹

$$k_{\text{eff}} = k_1 \frac{k_2[\text{HD}]}{k_2[\text{HD}] + k_{-1}} \quad (1)$$

SCHEME 1: Bergman Cyclization of (Z)-3-Ene-1,5-diyne



SCHEME 2: “Ortho Effect” in the Bergman Cyclization



In this paper we will apply density functional theory (DFT) to determine whether the influence of ortho substituents extends beyond the cyclization step to the kinetics and thermodynamics of H-atom abstraction in substituted *p*-naphthyne radicals. In principle, this influence can be transferred by two different mechanisms: (a) direct through-space interaction of incoming H-atom donor (in the TS) or hydrogen (in the product) with the substituent R and (b) by through-bond interaction of R with radical centers through the σ framework—an effect that is topologically identical to the through-bond interaction of nonbonding orbitals in 1,8- and 1,5-dehydronaphthalenes analyzed originally by Hoffmann^{22,39} and more recently by Squires and Cramer²³ (bold lines in Scheme 2) and to double hyperconjugation phenomenon in substituted cations²⁴ (vide infra). We will present a detailed theoretical study of geometries, electronic structure and energies of transition states and intermediates completing the full Bergman cycloaromatization pathway with the focus on polar and steric contributions to the kinetics and thermodynamics of hydrogen abstraction.

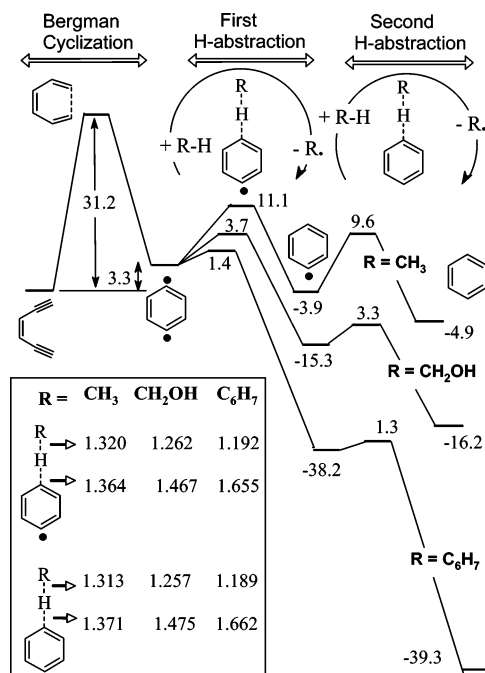
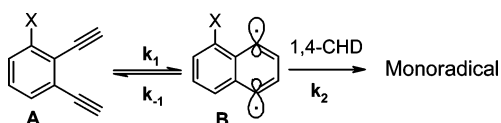


Figure 1. Reaction energy pathways for the successive hydrogen abstraction of *p*-benzyne by methane, methanol and 1,4-cyclohexadiene donors illustrated with the reaction barriers and energies (kcal/mol) along with the selected bond distances at the TS (UB3LYP/6-31G** level). All activation and reaction energies are given relative to the previous energy minimum.

SCHEME 3: Kinetic Model for the Bergman Cyclization of Ortho Substituted Enediyne



Computational Details

All monoradical and diradical geometries including transition states in hydrogen abstraction reactions were optimized at the UB3LYP/6-31G** level²⁵ using Gaussian 98 and 03 programs²⁶ whereas the restricted B3LYP/6-31G** method was used for the closed-shell systems. However, the broken-spin symmetry unrestricted B3LYP method was used for the diradical structures and also for the transition structures of the first hydrogen abstraction process. All $\langle S^2 \rangle$ values were less than 0.20 after the spin annihilation step (~ 0.96 before annihilation). The unrestricted MP2/6-31G** calculations were carried out for monoradical systems to cross-evaluate the DFT performance in the description of noncovalent interactions. Frequency calculations were performed to obtain thermochemical corrections to electronic energies, and to ensure that the geometries

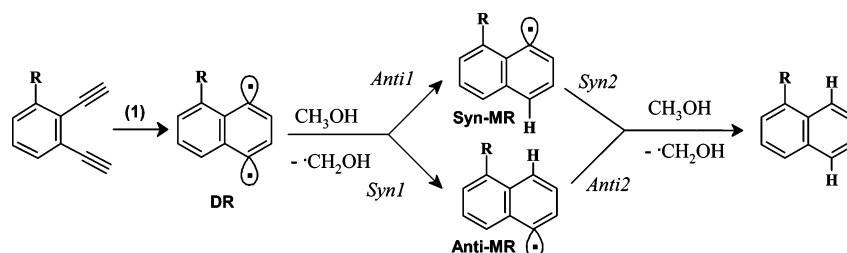
had been optimized to true minima. All structures contained the proper number of imaginary frequencies: zero for local minima and one along the mode of hydrogen abstraction for all transition states. Additionally, for several transition states the eigenvalue-following algorithm was used to remove spurious imaginary frequencies produced in optimizations using the default Berny algorithm. The NBO computations were carried out to analyze the electronic properties of diradical and radical systems using the NBO 4.0²⁷ that is implemented in Gaussian software.

Results and Discussion

Nature of H-Atom Donor. As a first step, we mapped potential energy surfaces for the reaction of the *p*-benzyne²⁸ and phenyl radicals with three H-atom donors of different reactivity (methane, methanol and 1,4-cyclohexadiene (CHD)) using BS-UB3LYP/6-31G** computations. As expected, the ability to donate a hydrogen atom increases in the order of CH₄ < CH₃OH < CHD, in parallel to the weakening of the C–H bonds (bond lengths of 1.092, 1.101 and 1.102 Å and BDE of 105, 92 and 73 kcal/mol²⁹ respectively, Figure 1). The relative position of the TS (late or early) in these reactions parallels reaction exothermicities in accord with the Leffler–Hammond postulate.³⁰ It is instructive to compare these DFT results with the results from the earlier work by Chen and co-workers who studied H-atom abstraction by *p*-benzyne and phenyl radicals from methanol at the CASPT2N/6-31G**//CAS/3-21G level and found the barriers to be 9.51 and 7.95 kcal/mol and incipient C...H distances of 1.375 and 1.275 Å, respectively.³¹ Although these barriers are noticeably higher than the 3.7 and 3.3 kcal/mol barriers for these processes at the UB3LYP/6-31G** level, it is possible that the advantage of high level multiconfigurational treatment is partially compromised by using the less accurate CAS (4×4) and CAS (3×3)/3-21G geometries and perhaps that UDFT gives a more balanced description of the whole process. Interestingly, when DFT and CASPT2N geometries are similar, the barriers calculated by the two methods are closer (e.g., the arene C...H DFT distance of 1.371 Å for methane/*p*-benzyne versus the CASPT2N distance of 1.375 Å for methanol/phenyl radical parallel the differences in the activation barriers (9.6 vs 9.5 kcal/mol). Such close correspondence is partially coincidental (the polar effects on TS should be different in the two cases) but does suggest that good geometries are essential for the description of such bond-breaking/bond-forming processes.

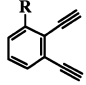
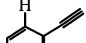
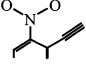
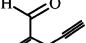
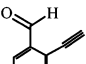
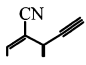
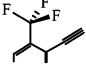
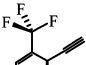
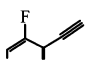
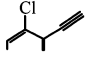
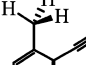
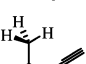
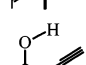
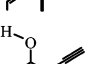
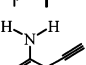
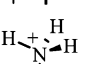
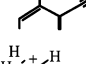
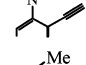
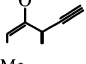
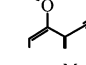
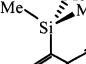
The second H-abstraction step is calculated to be roughly 1 kcal/mol less exothermic for all donors than the first step (the origin of this effect will be discussed later) but the extent to which this loss of exothermicity is translated to the activation barrier decrease is different. As the reactions become more exothermic, the difference between the barriers of first and

SCHEME 4: Four Possible H-atom Abstraction Steps in *p*-Benzyne Produced by the Bergman Cyclization of Ortho-Substituted Enediyne^a



^a DR = diradical, Syn-MR and Anti-MR = monoradicals with substituent R, respectively, “syn” and “anti” to the radical center.

TABLE 1: Reaction Energies (kcal/mol) for All Possible Steps in the Bergman Cycloaromatization Pathways of Ortho-Substituted Eneidyne (Parent (Z)-3-Ene-1,5-diyne Included for Comparison) at the UB3LYP/6-31G Level with CH₄ and CH₃OH (in Parentheses) as H-Atom Donors^a**

	R^b	ΔE (BC)		ΔE (Habs)			
		Bergman Cyclization	Anti1	Syn2	Syn1	Anti2	Anti1 + Syn2 or Syn1 + Anti2
	H	11.0	-3.9 (-15.0)	-4.9 (-16.4)	-3.9 (-15.0)	-4.9 (-16.4)	-8.8 (-31.4)
	NO ₂	6.6	-4.2 (-15.5)	-3.3 (-14.5)	-2.2 (-13.4)	-5.3 (-16.6)	-7.5 (-30.0)
	CHO (syn)	6.8	-3.8 (-15.0)	-4.7 (-16.0)	-3.4 (-14.6)	-5.1 (-16.4)	-8.5 (-31.0)
	CHO (anti)	9.4	-3.8 (-15.2)	-2.4 (-13.7)	-1.0 (-12.5)	-5.2 (-16.5)	-6.2 (-28.9)
	CN	10.0	-4.4 (-15.6)	-6.1 (-17.4)	-4.9 (-16.1)	-5.5 (-16.8)	-10.5 (-33.0)
	CF ₃ (st)	9.2	-4.1 (-15.3)	-5.1 (-16.4)	-3.9 (-15.1)	-5.3 (-16.6)	-9.2 (-31.7)
	CF ₃ (ec)	8.6	-4.0 (-15.3)	-3.4 (-14.7)	-2.2 (-13.5)	-5.2 (-16.5)	-7.4 (-30.0)
	F	10.8	-4.1 (-15.4)	-6.1 (-17.3)	-4.8 (-16.1)	-5.4 (-16.6)	-10.2 (-32.7)
	Cl	10.0	-4.3 (-15.5)	-5.2 (-16.5)	-4.2 (-15.5)	-5.3 (-16.5)	-9.5 (-32.0)
	CH ₃ (st)	10.9	-3.8 (-15.1)	-4.0 (-15.2)	-2.7 (-14.0)	-5.0 (-16.3)	-7.8 (-30.3)
	CH ₃ (ec)	11.0	-3.8 (-15.1)	-2.7 (-14.0)	-1.6 (-12.9)	-5.0 (-16.2)	-6.6 (-29.1)
	OH (syn)	12.8	-4.0 (-15.2)	-2.1 (-13.3)	-0.8 (-12.1)	-5.2 (-16.5)	-6.1 (-28.5)
	OH (anti)	10.6	-4.1 (-15.4)	-5.7 (-17.0)	-4.6 (-15.9)	-5.2 (-16.5)	-9.8 (-32.4)
	NH ₂	12.4	-3.9 (-15.1)	-2.1 (-13.4)	-1.0 (-12.2)	-5.0 (-16.3)	-6.0 (-28.5)
	NH ₃ ⁺ (st)	10.6	-5.5 (-16.8)	-3.3 (-14.6)	-1.9 (-13.2)	-7.0 (-18.2)	-8.8 (-31.4)
	NH ₃ ⁺ (ec)	11.7	-5.5 (-16.8)	-1.7 (-12.9)	-0.3 (-11.5)	-7.0 (-18.2)	-7.3 (-29.7)
	OMe (syn)	8.9	-3.8 (-15.0)	0.9 (-10.4)	2.0 (-9.3)	-4.9 (-16.2)	-2.9 (-25.4)
	OMe (anti)	10.3	-4.0 (-15.3)	-5.6 (-16.9)	-4.4 (-15.7)	-5.2 (-16.5)	-9.6 (-32.3)
	TMS (st)	9.7	-3.5 (-14.8)	-2.3 (-13.5)	-1.0 (-12.2)	-4.8 (-16.1)	-5.8 (-28.3)
	TMS (ec)	8.9	-3.5 (-14.8)	-1.8 (-13.0)	-0.6 (-11.8)	-4.7 (-16.0)	-5.3 (-27.8)

^a Separated molecules were used to calculate energies of starting materials and products. This choice eliminates complications due to formation of noncovalently bound complexes. ^b The staggered and eclipsed isomers (see above) are abbreviated as "st" and "ec", respectively.

TABLE 2: Estimates of TB Interaction between the Two Radical Centers through the Singlet–Triplet Gap and through the Difference between First and Second H-Atom Abstraction (Syn1–Syn2 = Anti1–Anti2) at the Same Position (Both in kcal/mol at the UB3LYP/6-31G level)**

R	S–T gap	BSE ^a = $E(\text{Syn1} - \text{Syn2})$ or $E(\text{Anti1} - \text{Anti2})^b$
NO ₂	2.44	1.10
CHO (syn)	2.89	1.38
CHO (anti)	3.01	1.40
CN	2.45	1.18
CF ₃ (st)	2.63	1.25
CF ₃ (ec)	2.58	1.18
H	2.72	1.33
F	2.57	1.25
Cl	2.22	0.99
CH ₃ (st)	2.59	1.21
CH ₃ (ec)	2.50	1.14
OH (syn)	2.66	1.23
OH (anti)	2.42	1.11
NH ₂	2.44	1.18
NH ₃ (st)	2.91	1.46
NH ₃ (ec)	2.95	1.41
OMe (syn)	2.63	1.15
OMe (anti)	2.43	1.18
TMS(st)	2.75	1.30
TMS (ec)	2.66	1.23

^a Biradical stabilization energies were obtained from the isodesmic equation in Scheme 5. ^b Subtracted energies of the H-abstraction processes (which is the same as the isodesmic equation in Scheme 5).

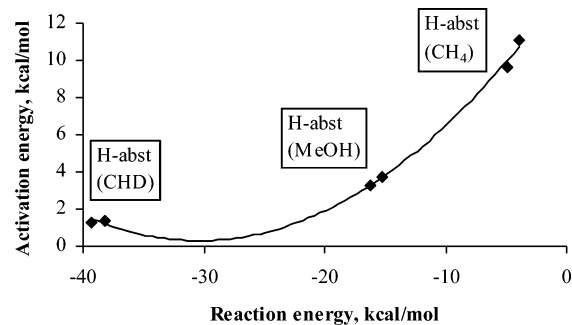


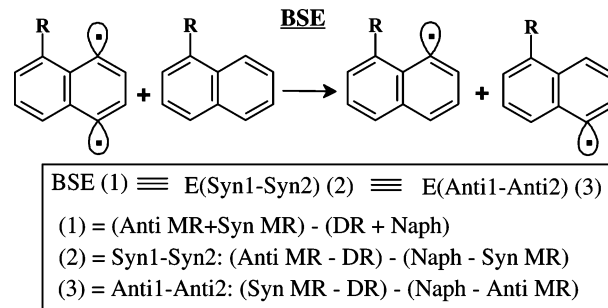
Figure 2. Correlation between calculated reaction energies and activation barriers (UB3LYP/6-31G**).

second H-abstractions decreases, suggesting that the dependence of reaction energies from the activation barriers is not linear and lies outside of the range where the Evans–Polanyi–Semenov correlation³² is applicable (Figure 2).³³

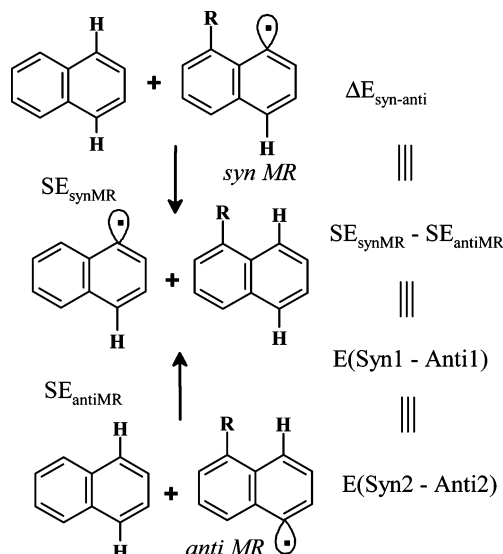
Nevertheless, one can compare trends in *relative* stabilities of substituted radicals using any of the above donors. All hydrogen abstractions from methane are ~11 kcal/mol less exothermic, whereas the reactions of 1,4-CHD are ca. 23 kcal/mol more exothermic than in the case of methanol. These differences compare favorably with the differences in respective BDEs (13 and 19 kcal/mol, respectively). Reaction energies discussed in the following sections are calculated for methanol and methane. The activation barriers will be calculated for H-abstraction from methane to minimize complications due to noncovalent interactions between radical and H-atom donor (hydrogen bonding, steric, etc).

Substitution in the Naphthalene Radicals. Analysis of computational results shows that although reaction energies of the two H-atom abstraction steps in 1,4-didehydronaphthalene are within 0.3 kcal/mol of analogous values for 1,4-dehydrobenzene, introduction of a substituent at the fifth position of the naphthalene ring leads to noticeable variations in these energies (from –16.8 to –9.3 kcal/mol for the first H-

SCHEME 5: Comparison of BSEs with Differences in Exothermicities of First and Second Hydrogen Abstractions at Both Sides of the Naphthalene Ring



SCHEME 6: Relations between Isodesmic Equations Defining Substituent Stabilization Energies in Syn and Anti Naphthyl Radicals



abstraction, from –17.4 to –10.4 kcal/mol for the second H-abstraction, and from –25.4 to –33.0 kcal/mol for the two combined steps). Where do these variations come from?

Substituent Effects on Exothermicity of H-Abstraction. Consideration of substituent effects³⁴ should answer two fundamental questions: (a) whether radicals are capable of interacting with remote substituents through a σ -framework (Scheme 2) via a double hyperconjugation mechanism, which is well-represented in the chemistry of cations^{24,35–38} and (b) whether through-space interaction of radicals with adjacent substituents is stabilizing or destabilizing.

In ortho-substituted enediynes, the two consecutive hydrogen abstraction steps that complete the Bergman cycloaromatization cascade are different from two perspectives (Scheme 4). On one hand, the first of the H-atom abstractions proceeds from a diradical, whereas the second abstraction proceeds from a monoradical. It is well-established that 1,4-diradicals are more selective and less reactive than the respective monoradicals (vide infra).³¹ On the other hand, the presence of an “ortho” substituent will make H-abstraction by the radical center that is adjacent to this substituent (referred to as “syn” abstraction in this paper) inherently different from abstraction by the radical center at the fifth carbon (referred to as “anti” abstraction). The “anti” abstraction in the diradical (the “Anti-1” process) produces a “syn” monoradical (“Syn-MR”) whereas the “syn” abstraction in the diradical (the “Syn-1” process) provides an “anti” monoradical (“Anti-MR”, Scheme 4). Reaction energies for all

TABLE 3: Substituent Effects on the Relative Stability of Syn and Anti Monoradicals^a

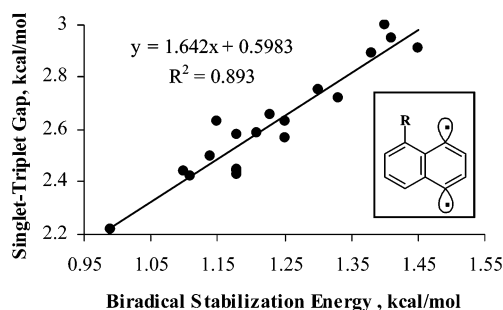
R	$\Delta E_{\text{syn-anti}},^b$ kcal/mol	$SE_{\text{synMR}},^c$ kcal/mol	$SE_{\text{antiMR}},^d$ kcal/mol
NO ₂	2.06 (1.78)	1.82	-0.25
CHO (syn)	0.42 (-0.24)	0.35	-0.06
CHO (anti)	2.75 (2.55)	2.65	-0.10
CN	-0.55 (-0.80)	-1.02	-0.46
CF ₃ (st)	0.21 (0.05)	-0.02	-0.23
CF ₃ (ec)	1.82 (1.60)	1.70	-0.12
H	0.00 (0.00)	0.00	0.00
F	-0.71 (-1.00)	-0.99	-0.28
Cl	0.02 (-0.21)	-0.15	-0.18
CH ₃ (st)	1.03 (0.77)	1.13	0.09
CH ₃ (ec)	2.23 (1.97)	2.34	0.11
OH (syn)	3.13 (2.80)	3.02	-0.11
OH (anti)	-0.53 (-1.01)	-0.64	-0.12
NH ₂	2.89 (2.39)	2.94	0.05
NH ₃ ⁺ (st)	3.63 (3.64)	1.74	-1.89
NH ₃ ⁺ (ec)	5.30 (5.21)	3.43	-1.87
OMe (syn)	5.74 (5.42)	5.93	0.19
OMe (anti)	-0.38 (-0.91)	-0.49	-0.12
TMS (st)	2.55	2.83	0.28
TMS (ec)	2.96	3.31	0.35

^a The relative energies (ΔE) and stabilization energies (SE) were computed at the UB3LYP/6-31G** and UMP2/6-31G** (values in parentheses) levels. If a $\Delta E_{\text{syn-anti}}$ value in Table 3 is negative, the anti radical is more stable than the respective syn radical. ^b The relative energies of syn and anti monoradicals (also equal to the $SE(\text{syn}) - SE(\text{anti})$ difference defined in Scheme 6. When they are negative, interaction of substituent R with the radical center is either less stabilizing or more destabilizing than interaction of the radical with R = H. Positive SEs mean that the presence of R stabilizes the system relative to the unsubstituted monoradical. ^c SE of syn monoradicals ($SE(\text{syn})$) defined in Scheme 6. ^d SE of anti monoradicals ($SE(\text{anti})$) defined in Scheme 6.

of the possible H-abstraction pathways are given in Table 1. We will analyze these data from both of the above-mentioned perspectives.

The energies of the four hydrogen abstractions are not independent. Because $\text{Syn1} + \text{Anti2} = \text{Anti1} + \text{Syn2}$ (the same product is formed), $\text{Syn1} - \text{Syn2} = \text{Anti1} - \text{Anti2}$, and thus, one can compare the first and the second H-abstraction from either side (two anti abstraction or two syn abstractions)—the result will be the same. For the same reason, $\text{Syn1} - \text{Anti1} = \text{Syn2} - \text{Anti2}$ and thus it does not make a difference whether one compares syn vs anti addition in diradicals or monoradicals.

(a) *Relative H-Abstraction Ability of Diradicals vs Monoradicals/Through-Bond Interaction of the Two Radical Centers.* The first interesting observation is that the differences in reaction energies between the Anti2 and Anti1 pathways (first and second H-abstractions from the side opposite to the substituent) and between the Syn2 and Syn1 pathways (first and second H-abstractions from the side adjacent to the substituent) consistently indicate that the first H-abstraction is always less exothermic than the second abstraction (Table 2). This observation is not surprising. Such differences in the energies of the first and second H-abstraction are known³¹ to originate from the orbital interaction of the two σ radicals through σ^* bridge orbitals (OITB: orbital interaction through-bonds).^{39a} This interaction, which is absent in monoradicals,^{23,31,40} provides an additional 3–5 kcal/mol of stabilization energy to the *p*-benzyne-type diradicals. Because this stabilizing energy is lost in the first H-atom abstraction, the *p*-benzyne diradicals are less reactive and more selective than simple phenyl radicals.³¹ Although the B3LYP values of TB interaction (1.0–1.5 kcal/mol) underestimate this effect, the results are qualitatively consistent with the earlier estimates. A very interesting and less

**Figure 3.** Correlation of two estimates of substituent effects on electronic coupling of radical centers in *p*-naphthylene diradicals at the UB3LYP/6-31G** level.

predictable finding is that the magnitude of this interaction depends on the substitution in the above *p*-benzynes. Although the absolute variations are small (ca. 0.5 kcal/mol), the *relative* magnitude of these changes in different molecules are significant (up to 50%). Interestingly, the $E(\text{Anti1}) - E(\text{Anti2})$ is the same as $E(\text{Syn1}) - E(\text{Syn2})$ and both of these values are *exactly* equal to the biradical stabilization energy (BSE) defined in Scheme 5 below.

The singlet–triplet (ST) gap provides an alternative estimate of OITB in these molecules because the stabilizing TB coupling of the two radical centers is absent in the triplet state. The UB3LYP values of the ST gap (2.4–3.1 kcal/mol) are in better agreement with the commonly accepted magnitude of OITB (3–5 kcal/mol) than the UB3LYP BSE energies. Although the range of values is relatively small and, thus, scattering is expected, the observed trends in the substituent effects⁴¹ from the two estimations correlate very well (Figure 3).

(b) *Polar and Steric Effects of Substituents.* The interaction of substituent R with the radical center can be estimated in two different ways. First, one can directly compare energies of the two substituted (syn and anti) monoradicals. A second and more informative way is to estimate relative stabilities of the two isomers of substituted radicals toward their unsubstituted analogue (the naphthyl radical). The isodesmic equations designed for these comparisons are shown in Scheme 6.

As expected, relative values of H-abstraction reaction energies by diradicals ($E(\text{A1})$ vs $E(\text{S1})$) or by monoradicals ($E(\text{A2})$ vs $E(\text{S2})$) are identical. In the case of bulky ortho substituents, one would expect introduction of a hydrogen atom instead of a radical center next to the substituent to be destabilizing and, thus, the respective $\Delta E_{\text{syn-anti}}$ value to be positive. This expectation is confirmed for X = NO₂ (2.1 kcal/mol), CH₃ (3.1 kcal/mol), syn-OH (3.1 kcal/mol) and especially, for X = NH₃. When NH₃⁺ is staggered, relative destabilization of the anti radical is 3.6 kcal/mol. Moreover, when the ammonium group attains an eclipsed conformation that puts one of the hydrogens next to the newly introduced H atom at the eighth position, the destabilization reaches its peak of 5.3 kcal/mol.

However, this simple steric interpretation does not explain why $\Delta E_{\text{syn-anti}}$ in the case of a relatively bulky staggered CF₃ group is only 0.2 kcal/mol. This value suggests that steric factors are partially compensated by a stabilizing factor. In the case of the Cl substituent, where $\Delta E_{\text{syn-anti}}$ is zero, the stabilizing and destabilizing effects almost perfectly compensate each other. Moreover, in the case of the σ acceptor substituents without considerable steric conflicts with H-8 (CN, F, anti-OH), the $\Delta E_{\text{syn-anti}}$ term is negative indicating larger stability of the “anti” radical. This stabilization reaches its maximum in the case of F (−0.7 kcal/mol).

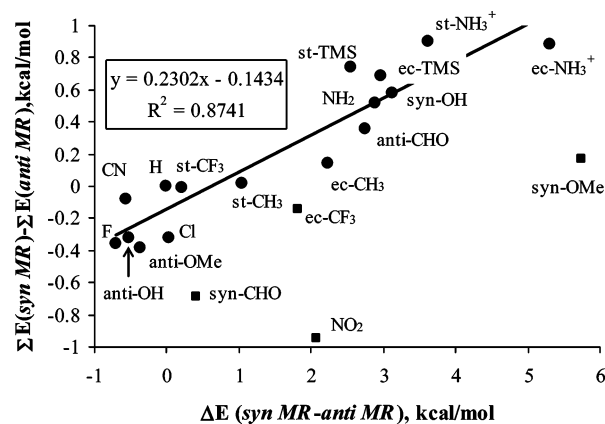


Figure 4. Correlation of the relative energy of syn and anti mono-radicals with the difference in the major interaction energies of both radicals (see also Scheme 7 and Table 4) calculated at the UB3LYP/6-31G** level. Data for those substituents that interact with the radical center directly through space (shown in red) deviate from the correlation.

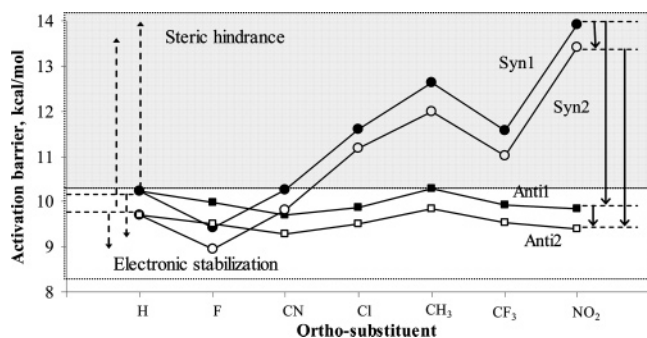
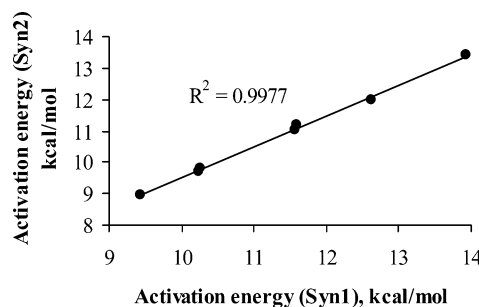


Figure 5. Trends in activation energies (UB3LYP/6-31G**) for syn and anti hydrogen abstractions involving substituted 1,4-didehydronaphthalenes.

To understand the nature of these effects, we determined the relative stabilities of substituted syn and anti mono-radicals separately using unsubstituted naphthyl 1-mono-radical as a reference. The results are given in the last two columns of Table 3. The range of SE (syn) values is greater because these values are influenced by direct through-space interaction of R and the radical center, which can be either stabilizing or destabilizing. Both effects can be quite significant (from -1 to $+3$ kcal/mol). Large positive numbers for the SE values for syn radicals result from a tradeoff between the stabilizing through-space interaction in the reactant and the steric interaction of the newly introduced H-atom and the substituent. However, in the case of strong σ acceptors without considerable steric interaction with the new C–H bond (CN, F, Cl, anti-OH and OMe), the SEs are negative, indicating the presence of a destabilizing factor in the syn mono-radical or a stabilizing factor in the final naphthalene product.



The SE values for anti radicals are smaller and mostly negative. Only Me and NH₂ provide very small positive numbers whereas most of the remaining values reveal a small destabilization, with the only exception being the large effect NH₃⁺ group (-1.9 kcal/mol). To get future insight into these effects, we added a stronger sigma donor (TMS) and found SE to be more positive. Obviously, these effects are purely electronic without a direct steric contribution. Negative values indicate that interaction of substituents at the first carbon with the anti radical center at the 8th carbon of naphthalene moiety provides *less* stabilization than the analogous interaction with a C–H bond.

Such destabilization by acceptor σ bonds reflects the electrophilic character of sp^2 -radicals. We investigated the nature of orbital interactions involving radicals and σ bonds using natural bond orbital (NBO) analysis. This analysis confirms the sensitivity of σ delocalizing interactions to the nature of syn and anti substituents. Because this picture is rather complex (we have shown only a part of the array of hyperconjugative interactions in Scheme 7), we restrict ourselves to a rather general discussion with the focus on donor/acceptor interactions involving radical orbitals. Such interactions are responsible for the “polar effects” important in radical reactivity.^{42,43}

Two orbital interactions were monitored for the diradicals where we analyzed the $\sigma(C-R) \rightarrow \sigma^*(C-C)$ (a) and $\sigma(C-C) \rightarrow \sigma^*(C-R)$ (a') interactions involving substituents R and the central C–C bond of the naphthalene moiety. In mono-radicals, the NBO analysis was extended to include the interactions of the central C–C bond with the radical center (b and b').⁴⁴ In every case, $a < b$ and $a' < b'$, which means that radicals are better donors and better acceptors than all C–R σ bonds in this paper. The balance between a and a' describes substituents as net donors or net acceptors. Only H and Me in this series can be considered as net donors but the balance of donor/acceptor ability of Me group is reversed by translocation of the radical center (syn vs anti). Interestingly, a similar increase in a' vs a is also observed in other anti mono-radicals. Comparison of b and b' is helpful in classifying the radicals as either nucleophilic ($b > b'$) or electrophilic ($b < b'$). Remarkably, in all of the syn mono-radicals (except for R = NO₂), the acceptor b' interaction prevails, suggesting that the radical center in these species should be viewed as electrophilic. The situation is less clear-cut in many of anti radicals where donation from the bridge σ -orbital to the radical center (b') decreases, rendering b greater than b' . Comparison of b_{syn} with b_{anti} shows how substitution perturbs donor ability of the radical orbital ($b_{syn} < b_{anti}$ for all of the cases except when R = F). Further interesting observations include conformational effects on σ delocalization, such as rebalancing of a/a' and b/b' interactions upon rotation of the OMe moiety in both syn and anti isomers.

The overall array of interactions is rather complicated but interestingly the difference in the combined magnitude of interactions given in Table 4 correlates with the difference in

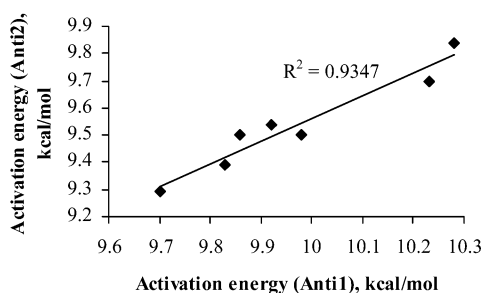


Figure 6. Correlation between Syn1 and Syn2 barriers as well as Anti1 and Anti2 barriers calculated from the hydrogen abstractions of ortho-substituted 1,4-didehydronaphthalene at the UB3LYP/6-31G** level.

TABLE 4: Second Order Perturbation Energies (kcal/mol) for the Interactions Shown in Scheme 7 from the NBO Calculations at the UB3LYP/6-31G Level**

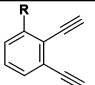
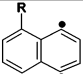
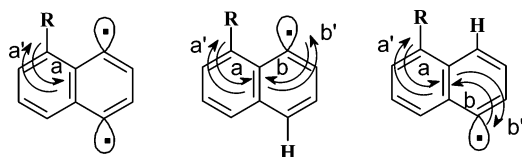
	Diradical (Singlet)		Diradical (Triplet)		Monoradical (syn)				Monoradical (anti)			
	a	a'	a	a'	a	a'	b	b'	a	a'	b	b'
NO ₂	1.79	4.45	1.69	4.38	1.72	4.27	5.69	5.59	1.38	5.04	6.17	5.63
CHO (syn)	2.83	2.86	2.79	2.85	2.71	2.77	5.69	5.65	2.34	3.13	5.99	6.05
CHO (anti)	2.83	2.86	2.67	2.81	2.84	2.73	5.69	6.58	2.39	3.09	6.04	5.96
CN	2.82	2.74	2.72	2.74	2.77	2.70	5.77	6.04	2.59	2.84	5.94	5.99
CF ₃ (st)	2.75	3.09	2.63	3.02	2.66	2.97	5.70	6.21	2.38	3.22	6.02	5.93
CF ₃ (ec)	2.46	3.54	2.35	3.47	2.38	3.41	5.66	6.17	2.01	3.88	6.13	5.74
H	4.38	1.93	4.23	1.96	4.37	1.91	5.73	6.32	4.37	1.91	6.50	6.32
F	1.71	3.78	1.64	3.75	1.66	3.67	5.88	6.06	1.64	3.91	5.85	6.23
Cl	2.69	4.33	2.61	4.32	2.62	4.27	5.84	6.06	2.43	4.67	5.99	6.02
CH ₃ (st)	3.09	2.74	2.95	2.73	2.98	2.67	5.62	6.51	2.75	2.90	5.95	6.16
CH ₃ (ec)	3.05	2.83	2.95	2.83	2.95	2.76	5.61	6.57	2.58	3.14	6.01	6.02
OH(syn)	1.65	3.42	1.58	3.41	1.61	3.33	5.78	7.12	1.42	3.87	5.96	6.01
OH(anti)	1.84	3.11	1.77	3.09	1.78	3.03	5.78	6.04	1.71	3.22	5.84	6.18
NH ₂	1.86	2.94	1.77	2.93	1.81	2.88	5.74	6.87	1.58	3.28	5.92	6.00
NH ₃ ⁺ (st)	1.92	4.85	1.83	4.86	1.86	4.70	6.04	7.03	1.65	5.35	6.21	5.52
NH ₃ ⁺ (ec)	1.93	4.77	1.84	4.80	1.87	4.64	5.91	7.42	1.55	5.71	6.28	5.42
OMe(syn)	1.25	4.44	1.18	4.45	1.24	4.37	5.52	7.04	1.07	5.13	6.14	5.66
OMe(anti)	1.86	2.98	1.77	2.97	1.80	2.90	5.72	6.04	1.71	3.12	5.86	6.15
TMS (st)	5.80	2.71	5.69	2.69	5.75	2.64	5.55	6.91	5.20	2.79	6.05	6.07
TMS (ec)	5.69	2.84	5.43	2.80	5.48	2.76	5.59	6.77	4.87	2.95	6.08	6.01

TABLE 5: Energy, Enthalpy and Free Energy of Activations (kcal/mol) for the Subsequent Hydrogen Abstractions of Ortho-Substituted 1,4-Didehydronaphthalene with CH₄ Donor (UB3LYP/6-31G) Based on the Syn and Anti Approaches Shown in Scheme 4**

	Syn1			Anti1			Syn2			Anti2		
	E _a	ΔH [‡]	ΔG [‡]	E _a	ΔH [‡]	ΔG [‡]	E _a	ΔH [‡]	ΔG [‡]	E _a	ΔH [‡]	ΔG [‡]
NO ₂	13.93	11.37	20.30	9.83	7.18	12.88	13.41	10.79	19.72	9.39	6.65	14.94
CF ₃	11.58	9.06	18.60	9.92	7.27	15.63	11.01	8.41	17.88	9.54	6.77	14.95
CN	10.27	7.73	16.24	9.70	7.06	15.38	9.82	7.18	15.66	9.29	6.56	14.87
H	10.23	7.54	15.73	10.23	7.54	15.73	9.70	8.12	15.92	9.70	8.12	15.92
F	9.43	6.75	15.01	9.98	7.29	15.38	8.94	6.16	14.30	9.50	6.74	14.82
Cl	11.60	9.01	17.76	9.86	7.18	15.50	11.19	8.55	17.36	9.50	6.76	15.07
CH ₃	12.63	10.13	19.00	10.28	7.55	15.60	11.98	9.46	18.58	9.84	7.05	15.16

SCHEME 7: Nature of Interactions Involved in the Diradicals and Monoradicals of Naphthalene Derivatives

absolute energies of syn and anti monoradicals (Figure 4). Although the slope of this correlation suggests that only one-fourth of the $\Delta E_{\text{syn-anti}}$ value comes directly from hyperconjugation, this correlation confirms that difference in stabilities reflect the fundamental interaction patterns between σ substituents in the naphthalene network whereas the deviation of $R = \text{NO}_2$ and syn-OMe substituted radicals from the correlation illustrates how the above σ effects can be attenuated by direct through-space interactions with sterically bulky substituents.

Substituent Effects on Transition States. Below, we will discuss electronic and steric effects of the ortho substituents on activation barriers for hydrogen abstraction from the same two perspectives as above: (a) diradical vs monoradical and (b) syn vs anti abstraction. The data are summarized in Table 5 and Figure 5.

(a) *Diradical vs Monoradical.* The computed activation barriers in Table 5 confirm that the first hydrogen abstraction

of ortho-substituted 1,4-didehydronaphthalene should proceed slower than the second abstraction on the same side, as reported earlier for other *p*-benzynes.^{31,45} The activation energy differences (0.4–0.7 kcal/mol) (Figure 5) are probably slightly underestimated at the UDFT levels. Energies of the first and second H-abstractions correlate well with each other (Figure 6). The correlation is slightly more scattered for the anti abstraction but mostly likely only because of the narrower range of data. Geometric parameters given in Figure 7 illustrate that more exothermic second abstractions (Syn2 and Anti2) proceed via earlier TS than the first abstractions (Syn1 and Anti1) in accord with the Leffler-Hammond postulate.³⁰

(b) *Syn and Anti Selectivity for Hydrogen Abstraction.* Computations reveal that hydrogen abstractions generally proceed faster via anti attack (Table 5). There are two main factors controlling the regioselectivity: (i) the *electronic effect* of substituents, which is displayed clearly in the “anti approach”, and (ii) the *steric hindrance* imposed by the substituents proximal to the incoming donor in the “syn approach”. The interplay of steric and electronic effects on the relative barriers along the syn and anti pathways is illustrated in Figure 5. In general, syn abstraction is more sensitive to substituents and the activation energy for the syn processes varies from 9 to 14 kcal/mol whereas for the anti it remains within the narrow range of 9.3–10.3 kcal/mol.

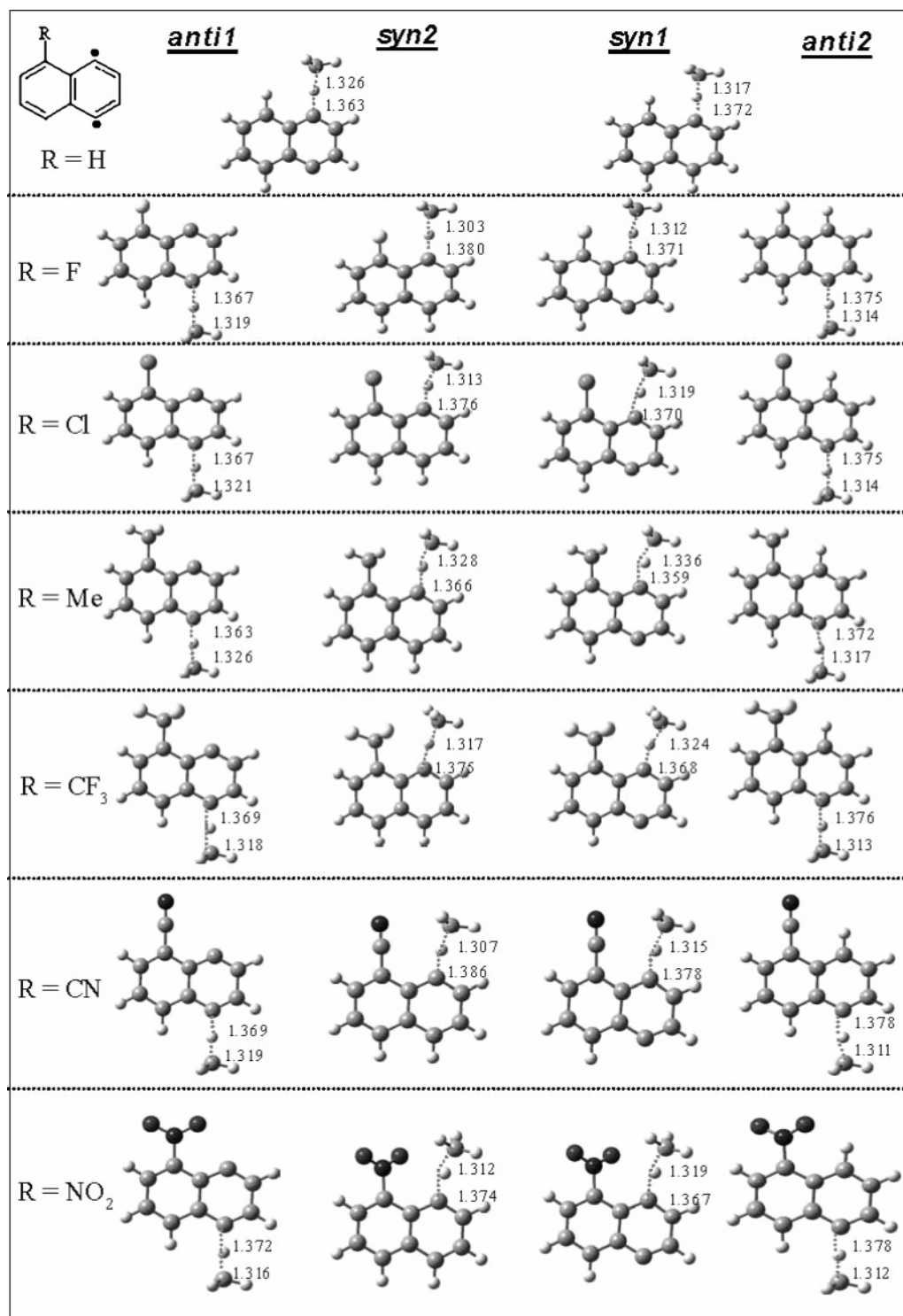


Figure 7. Selected distances for hydrogen abstractions by substituted 1,4-didehydronaphthalenes calculated at UB3LYP/6-31G** level.

(i) Syn Abstraction. On syn abstraction, the steric repulsion between incoming H-donor and ortho substituent increases in the order $H < F < CN < Cl < CH_3 < CF_3 < NO_2$, parallel to the increase in van der Waals radii of these groups.⁴⁶ The magnitude of this steric interaction can be estimated from the “deflection angle”⁴⁷ illustrated in Figure 8, which shows deviation of the H-donor approach from the ideal trajectory.

Figure 8 also illustrates the increase in the activation barrier due to the steric destabilization. This effect is particularly large for the nitro substituent where interaction with the incoming methane molecule results in 36° rotation of the NO₂ group (see

Figure 7) out of plane and partial disruption of conjugation with the aromatic moiety. However, interaction of H-donor and substituent is not limited to the steric repulsion. This is especially apparent in the case of F, CN and CF₃ groups where the activation energy is lower than one may expect from the deflection angle due to an attractive (C–H hydrogen bond) interaction.

(ii) Anti Abstraction. Obviously, the above steric effects do not apply in this case and electronic effects of substituents become easily observable. Interestingly, electron acceptors lower the activation barrier in the order $(CH_3 > H > F > Cl > CF_3$

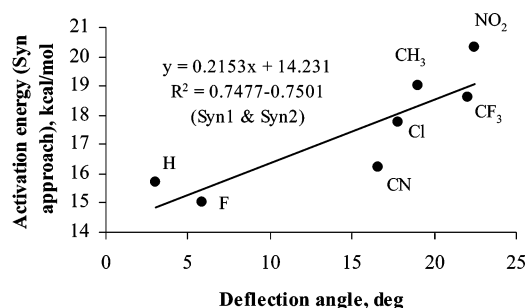
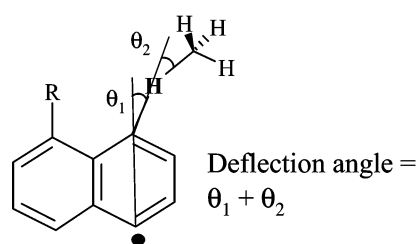


Figure 8. Definition of “deflection angle” (see Supporting Information for data) in the transition structures along with the correlation of these angles with the activation barriers for the syn hydrogen abstractions at the UB3LYP/6-31G** level.

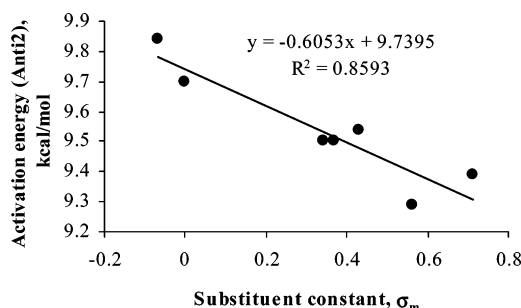
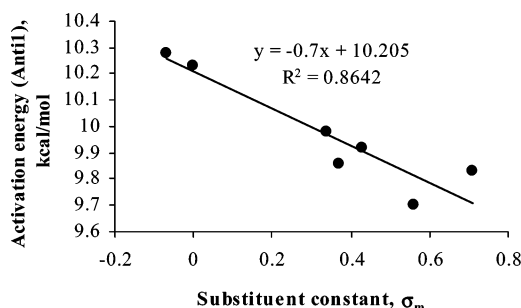


Figure 9. Correlation between Hammett constants (σ_m) and the activation barriers for the anti type hydrogen abstractions at the UB3LYP/6-31G** level.

> CN > NO₂) that parallels increase in the Hammett constants σ_m . The effects are not large (within 1 kcal/mol) but still remarkable because they provide a rare example of remote substitution that is capable of fine-tuning reactivity of a neutral reactive intermediate through a σ framework. Because the correlation coefficient for activation energies in Figure 9 is negative, the Hammett reaction constant (ρ) for reaction rates will be positive indicating increase in electron density at the reaction site that is consistent with electrophilic character of sp²-hybridized radicals.^{42a,48} Furthermore, inspection of C–H bonds formed and cleaved at the TS (Figure 7) suggests a shift to the earlier transition states upon an increase in the electron acceptor power of the substituents.

Conclusions

Two mechanisms are responsible for the effect of ortho substituents on the rate of H-atom abstraction from *p*-naphthylene diradicals formed in the Bergman cyclization of ortho-substituted enediyne. Direct through-space interaction of incoming H-atom donor with the substituent is important for the syn hydrogen abstraction. Reaction rates of anti H-abstractions are controlled by electronic effects based on through-bond interaction of R with radical centers. Hammett analysis indicates an increase in electron density at the radical in the transition state for the anti abstractions, which is consistent with electrophilic character of aryl radicals. Overall, this study provides a rare unambiguous example of remote substitution that affects reactivity of a neutral reactive intermediate through a σ framework.

Acknowledgment is made to Research Corporation, to the National Institutes of Health, and to Hamilton College for support of this work. This project was supported in part by NSF Grant CHE-0457275, and by NSF grants CHE-0116435 and CHE-0521063 as part of the MERCURY high-performance computer consortium (<http://mercury.chem.hamilton.edu>). I.A. is grateful to the National Science Foundation (CHE-0316598) for partial support of this research, to the 3M Company for an

Untenured Faculty Award and NCSA Supercomputing Center (award CHE050004N) for a generous allocation of computer time.

Supporting Information Available: Tables of relative energies, stabilization energies, deflection angles, atomic coordinates, and thermal energies. This material is available free of charge via the Internet at <http://pubs.acs.org>.

References and Notes

- (1) Jones, R. R.; Bergman, R. G. *J. Am. Chem. Soc.* **1972**, *94*, 660. Bergman, R. G. *Acc. Chem. Res.* **1973**, *6*, 25–31.
- (2) (a) *Enediyne Antibiotics as Antitumor Agents*; Borders, D. B., Doyle, T. W., Eds.; Marcel Dekker: New York, 1995. (b) *Neocarzinostatin: The Past, Present, and Future of an Anticancer Drug*; Maeda, H., Edo, K., Ishida, N., Eds.; Springer, New York, 1997.
- (3) Wu, M.; Stoermer, D.; Tullius, T.; Townsend, C. A. *J. Am. Chem. Soc.* **2000**, *122*, 12884.
- (4) The Bergman reaction as a synthetic tool: Bowles, D. M.; Palmer G. J.; Landis, C. A.; Scott, J. L.; Anthony, J. E. *Tetrahedron* **2001**, *57*, 3753. Bowles, D. M.; Anthony, J. E. *Org. Lett.* **2000**, *2*, 85.
- (5) Chen, X.; Tolbert, L. M.; Hess, D. W.; Henderson, C. *Macromolecules* **2001**, *34*, 4104. Shah, H. V.; Babb, D. A.; Smith, D. W., Jr. *Polymer* **2000**, *41*, 4415. John, J. A.; Tour, J. M. *J. Am. Chem. Soc.* **1994**, *116*, 5011.
- (6) Incorporation of the enediyne unit into a strained 9- or 10-membered ring was shown to facilitate the reaction through ground-state destabilization. Alabugin, I. V.; Manoharan, M. *J. Phys. Chem. A* **2003**, *107*, 3363. For the selected experimental work see: (a) Nicolaou, K. C.; Zuccarello, G.; Ogawa, Y.; Schweiger, E. J.; Kumazawa, T. *J. Am. Chem. Soc.* **1988**, *110*, 4866. (b) Nicolaou, K. C.; Zuccarello, G.; Riemer, C.; Estevez, V. A.; Dai, W.-M. *J. Am. Chem. Soc.* **1992**, *114*, 7360. (c) Iida, K.; Hiram, M. *J. Am. Chem. Soc.* **1995**, *117*, 8875.
- (7) For a theoretical analysis of the strain effects on the cyclization see: Snyder, J. P. *J. Am. Chem. Soc.* **1989**, *111*, 7630. Snyder, J. P.; Tipsword, G. E. *J. Am. Chem. Soc.* **1990**, *112*, 4040. Snyder, J. P. *J. Am. Chem. Soc.* **1990**, *112*, 5367.
- (8) Kraka, E.; Cremer, D. *J. Am. Chem. Soc.* **1994**, *116*, 4929.
- (9) The cyclization can also be controlled by release of strain in the transition state: Magnus, P.; Carter, P.; Elliott, J.; Lewis, R.; Harling, J.; Pittner, T.; Bauta, W. E.; Fortt, S. *J. Am. Chem. Soc.* **1992**, *114*, 2544.
- (10) For recent reviews, see: Rawat, D. S.; Zaleski, J. M. *Synlett* **2004**, 393. Klein, M.; Walenzyk, T.; König, B. *Collect. Czech. Chem. Commun.* **2004**, *69*, 945. Basak, A.; Mandal, S.; Bag, S. S. *Chem. Rev.* **2003**, *103*, 4077.

- (11) Schmittel, M.; Kiau, S. *Chem. Lett.* **1995**, 953.
- (12) Mayer, M. E.; Greiner, B. *Lieb. Ann. Chem.* **1992**, 855.
- (13) Choy, N.; Kim, C.-S.; Ballester, C.; Argitas, L.; Diez, C.; Lichtenberg, F.; Shapiro, J.; Russell, K. C. *Tetrahedron Lett.* **2000**, 41, 6995. Correlation of the reaction rate with Hammett σ_m value revealed a low sensitivity to substituents ($\rho = 0.654$). The Swain–Lupton model yielded a larger field parameter (0.662) than the resonance parameter (0.227), indicating that conjugative effects in the out-of-plane π -system are of lesser importance than field effects.
- (14) Jones, G. B.; Plourde, G. W. *Org. Lett.* **2000**, 2, 1757. Jones, G. B.; Warner, P. M. *J. Am. Chem. Soc.* **2001**, 123, 2134. Plourde, G. W., II; Warner, P. M.; Parrish, D. A.; Jones, G. B. *J. Org. Chem.* **2002**, 67, 5369. Jones, G. B.; Wright, J. M.; Hynd, G.; Wyatt, J. K.; Warner, P. M.; Huber, R. S.; Li, A.; Kilgore, M. W.; Sticca, R. P.; Pollenz, R. S. *J. Org. Chem.* **2002**, 67, 5727.
- (15) Haberhauer, G.; Gleiter, R. *J. Am. Chem. Soc.* **1999**, 121, 4664.
- (16) Galbraith, J. M.; Schreiner, P. R.; Harris, N.; Wei, W.; Wittkopp, A.; Shaik, S. *Chem. Eur. J.* **2000**, 6, 1446.
- (17) Alabugin, I. V.; Manoharan, M.; Kovalenko, S. V. *Org. Lett.* **2002**, 4, 1119.
- (18) Decrease in retro-Bergman barrier for benzannelated enediyne: Haberhauer, G.; Gleiter, R. *J. Am. Chem. Soc.* **1999**, 121, 4664. Koseki, S.; Fujimura, Y.; Hiram, M. *J. Phys. Chem.* **1999**, 103, 7672. Stahl, F.; Moran, D.; Schleyer, P. v. R.; Prall, M.; Schreiner, P. R. *J. Org. Chem.* **2002**, 67, 1453.
- (19) Kaneko, T.; Takahashi, M.; Hiram, M. *Tetrahedron Lett.* **1999**, 40, 2015.
- (20) For a recent discussion of such kinetic complications, see: Semmelhack, M. F.; Sarpong, R. *J. Phys. Org. Chem.* **2004**, 17, 807.
- (21) Zeidan, T.; Manoharan, M.; Alabugin, I. V. *J. Org. Chem.* **2006**, 71, 954. Zeidan, T.; Kovalenko, S. V.; Manoharan, M.; Alabugin, I. V. *J. Org. Chem.* **2006**, 71, 962.
- (22) Theoretical analysis of orbital interactions involving σ -bonds: Alabugin, I. V.; Zeidan, T. A. *J. Am. Chem. Soc.* **2002**, 124, 3175. Alabugin, I. V. *J. Org. Chem.* **2000**, 65, 3910.
- (23) Electronic interactions in didronaphthalene biradicals. Squires, R. R.; Cramer, C. J. *J. Phys. Chem. A* **1998**, 102, 9072.
- (24) Alabugin, I. V.; Manoharan, M. *J. Org. Chem.* **2004**, 69, 9011.
- (25) (a) Becke, A. D. *Phys. Rev. A* **1988**, 38, 3098. (b) Lee, C. T.; Yang, W. T.; Parr, R. G. *Phys. Rev. B* **1988**, 37, 785. (c) Stephens, P. J.; Devlin, F. J.; Chabalowski, C. F.; Frisch, M. J. *J. Phys. Chem.* **1994**, 98, 11623.
- (26) Frisch, M. J.; Trucks, G. W.; Schlegel, H. B.; Scuseria, G. E.; Robb, M. A.; Cheeseman, J. R.; Zakrzewski, V. G.; Montgomery, J. A., Jr.; Stratmann, R. E.; Burant, J. C.; Dapprich, S.; Millam, J. M.; Daniels, A. D.; Kudin, K. N.; Strain, M. C.; Farkas, O.; Tomasi, J.; Barone, V.; Cossi, M.; Cammi, R.; Mennucci, B.; Pomelli, C.; Adamo, C.; Clifford, S.; Ochterski, J.; Petersson, G. A.; Ayala, P. Y.; Cui, Q.; Morokuma, K.; Malick, D. K.; Rabuck, A. D.; Raghavachari, K.; Foresman, J. B.; Cioslowski, J.; Ortiz, J. V.; Stefanov, B. B.; Liu, G.; Liashenko, A.; Piskorz, P.; Komaromi, I.; Gomperts, R.; Martin, R. L.; Fox, D. J.; Keith, T.; Al-Laham, M. A.; Peng, C. Y.; Nanayakkara, A.; Gonzalez, C.; Challacombe, M.; Gill, P. M. W.; Johnson, B. G.; Chen, W.; Wong, M. W.; Andres, J. L.; Head-Gordon, M.; Replogle, E. S.; Pople, J. A. *Gaussian 98*, revision A.9; Gaussian, Inc.: Pittsburgh, PA, 1998. Frisch, M. J.; Trucks, G. W.; Schlegel, H. B.; Scuseria, G. E.; Robb, M. A.; Cheeseman, J. R.; Montgomery, J. A., Jr.; Vreven, T.; Kudin, K. N.; Burant, J. C.; Millam, J. M.; Iyengar, S. S.; Tomasi, J.; Barone, V.; Mennucci, B.; Cossi, M.; Scalmani, G.; Rega, N.; Petersson, G. A.; Nakatsuji, H.; Hada, M.; Ehara, M.; Toyota, K.; Fukuda, R.; Hasegawa, J.; Ishida, M.; Nakajima, T.; Honda, Y.; Kitao, O.; Nakai, H.; Klene, M.; Li, X.; Knox, J. E.; Hratchian, H. P.; Cross, J. B.; Bakken, V.; Adamo, C.; Jaramillo, J.; Gomperts, R.; Stratmann, R. E.; Yazyev, O.; Austin, A. J.; Cammi, R.; Pomelli, C.; Ochterski, J. W.; Ayala, P. Y.; Morokuma, K.; Voth, G. A.; Salvador, P.; Dannenberg, J. J.; Zakrzewski, V. G.; Dapprich, S.; Daniels, A. D.; Strain, M. C.; Farkas, O.; Malick, D. K.; Rabuck, A. D.; Raghavachari, K.; Foresman, J. B.; Ortiz, J. V.; Cui, Q.; Baboul, A. G.; Clifford, S.; Cioslowski, J.; Stefanov, B. B.; Liu, G.; Liashenko, A.; Piskorz, P.; Komaromi, I.; Martin, R. L.; Fox, D. J.; Keith, T.; Al-Laham, M. A.; Peng, C. Y.; Nanayakkara, A.; Challacombe, M.; Gill, P. M. W.; Johnson, B. G.; Chen, W.; Wong, M. W.; Gonzalez, C.; Pople, J. A. *Gaussian 03*, revision C.02; Gaussian, Inc.: Wallingford, CT, 2004.
- (27) Glendening, E. D.; Badenhoop, J. K.; Reed, A. E.; Carpenter, J. E.; Weinhold, F. *NBO 4.0*; Theoretical Chemistry Institute, University of Wisconsin: Madison, WI, 1996.
- (28) Clark, A. E.; Davidson, E. R. *J. Phys. Chem. A* **2002**, 106, 6890.
- (29) Wanger, D. D. M.; Giller, D. *Adv. Free Rad. Chem.* **1990**, 1, 159.
- (30) Leffler, J. E. *Science* **1953**, 117, 340. Hammond, G. S. *J. Am. Chem. Soc.* **1955**, 77, 334.
- (31) Logan, C. F.; Chen, P. *J. Am. Chem. Soc.* **1996**, 118, 2113.
- (32) Schottelius, M. J.; Chen, P. *J. Am. Chem. Soc.* **1996**, 118, 4896.
- (33) Bell, R. P. *Proc. R. Soc. London, Ser. A* **1936**, 154, 414. Evans, M. G.; Polanyi, M. *Trans. Faraday Soc.* **1938**, 34, 11.
- (34) Alabugin, I. V.; Manoharan, M.; Breiner, B.; Lewis, F. D. *J. Am. Chem. Soc.* **2003**, 125, 9329.
- (35) Nash, J. J.; Nizzi, K. E.; Adeyua, A.; Yurkovich, M. J.; Cramer, C. J.; Kenttämä, H. I. *J. Am. Chem. Soc.* **2005**, 127, 5760. Amegayibor, F. S.; Nash, J. J.; Kenttämä, H. I. *J. Am. Chem. Soc.* **2003**, 1257, 14256. Amegayibor, F. S.; Nash, J. J.; Lee, A. S.; Thoen, J.; Petzold, C. J.; Kenttämä, H. I. *J. Am. Chem. Soc.* **2002**, 124, 12066.
- (36) Grob, C. A.; Rich, R. *Tetrahedron* **1978**, 29, 663.
- (37) Lambert, J. B.; Ciro, C. M. *J. Org. Chem.* **1996**, 61, 1940.
- (38) This phenomenon is particularly important for Si and Sn-organic compounds where it is called the δ effect: (a) Lambert, J. B.; Salvador, L. A.; So, J.-H. *Organometallics* **1993**, 12, 697. (b) Adcock, W.; Coope, J.; Shiner, V. J., Jr.; Trout, N. A. *J. Org. Chem.* **1990**, 55, 1411. (c) Adcock, W.; Kristic, A. R.; Duggan, P. J.; Shiner, V. J., Jr.; Coope, J.; Ensinger, M. W. *J. Am. Chem. Soc.* **1990**, 112, 3140. (d) Lambert, J. B.; Salvador, L. A. *Tetrahedron Lett.* **1990**, 31, 3841. (e) Green, A. J.; Van, V.; White, J. M. *Aust. J. Chem.* **1998**, 51, 555. See also: Adcock, W.; Cotton, J.; Trout, N. A. *J. Org. Chem.* **1994**, 59, 1867. Adcock, W.; Head, N. J.; Lokan, N. R.; Trout, N. A. *J. Org. Chem.* **1997**, 62, 6177.
- (39) Selected theoretical studies: Hrovat, D. A.; Borden, W. T. *J. Org. Chem.* **1992**, 57, 2519.
- (40) (a) Hoffman, R.; Imamura, A.; Hehre, W. J. *J. Am. Chem. Soc.* **1968**, 90, 1499. Hoffman, R. *Acc. Chem. Res.* **1971**, 4, 1. (b) Paddon-Row, M. N. *Acc. Chem. Res.* **1982**, 15, 245. (c) Gleiter, R.; Schafer, W. *Acc. Chem. Res.* **1990**, 23, 369–375. (d) Brodskaya, E. I.; Ratovskii, G. V.; Voronkov, M. G. *Russ. Chem. Rev.* **1993**, 62, 975.
- (41) Kraka, E.; Cremer, D. *J. Am. Chem. Soc.* **2000**, 122, 8245.
- (42) Johnson, W. T. G.; Cramer, C. J. *J. Am. Chem. Soc.* **2001**, 123, 923. Clark, A. E.; Davidson, E. R. *J. Org. Chem.* **2003**, 68, 3387.
- (43) (a) Alabugin, I. V.; Manoharan, M. *J. Am. Chem. Soc.* **2005**, 127, 9534. For the recent work see: (a) Alabugin, I. V.; Manoharan, M. *J. Am. Chem. Soc.* **2005**, 127, 9534 and references therein. Also: (b) Lalevée, J.; Allonas, X.; Fouassier, J.-P. *J. Org. Chem.* **2005**, 70, 814. (c) Weber, M.; Fischer, H. H. *Helv. Chim. Acta* **1998**, 81, 770. (d) Beckwith, A. L. J.; Poole, J. S. *J. Am. Chem. Soc.* **2002**, 124, 9489. (e) Zytowski, T.; Kneuhl, B.; Fischer, H. *Helv. Chim. Acta* **2000**, 83, 658. (f) Heberger, K.; Lopata, A. *J. Org. Chem.* **1998**, 63, 8646. (g) Zytowski, T.; Fischer, H. *J. Am. Chem. Soc.* **1996**, 118, 437. (h) Batchelor, S. N.; Fischer, H. *J. Phys. Chem.* **1996**, 100, 9794. (i) Walbinder, M.; Fischer, H. *J. Phys. Chem.* **1993**, 97, 4880. (j) Martschke, R.; Farley, R. D.; Fischer, H. *Helv. Chim. Acta* **1997**, 80, 1363. (k) Lalevée, J.; Allonas, X.; Fouassier, J.-P. *J. Phys. Chem. A* **2004**, 108, 4326.
- (44) The SOMO-LUMO interaction: Park, S. U.; Chung, S. K.; Newcomb, M. *J. Am. Chem. Soc.* **1986**, 108, 240. The SOMO–HOMO interaction: Avila, David V.; Ingold, K. U.; Luszyk, J.; Dolbier, W. R.; Pan, H. Q. *J. Am. Chem. Soc.* **1993**, 115, 1577. Hartung, J.; Kneuer, R.; Rummey, C.; Bringmann, G. *J. Am. Chem. Soc.* **2004**, 126, 12121.
- (45) Coupling of radical centers complicates NBO analysis of b and b' interactions in the singlet *p*-benzyne diradicals.
- (46) Hiram, M. *Pure Appl. Chem.* **1997**, 69, 525.
- (47) Bondi, A. *J. Phys. Chem.* **1964**, 68, 441. Pauling, L. *The Nature of the Chemical Bond*, 3rd ed.; Cornell University Press: Ithaca, NY, 1960.
- (48) The angle of deflection is calculated from the sum of angles that are deviated from the perpendicular axes (which originate from the C1 and C4 atoms) where donor system approaches at the TS.
- (49) Alabugin, I. V.; Manoharan, M. *J. Am. Chem. Soc.* **2005**, 127, 12583. and references therein.